

## A APPENDIX

### A.1 OVERVIEW

In this supplementary material, we provide the pseudo-code for **CoINR**, along with a detailed explanation of the activation function selection process for both the image and occupancy fields. Additionally, we present qualitative results for each configuration mentioned in the main paper, allowing for a clearer understanding of the model’s performance across different scenarios. Lastly, we include guidelines for selecting the value of the hyperparameter  $s$ , which plays a key role in optimizing the model’s performance. These materials are intended to complement the main text, offering further insights into the flexibility and effectiveness of **CoINR**.

### A.2 PSEUDOCODE OF **CoINR**

The following algorithm provides the pseudo code for **CoINR**

---

#### Algorithm 1 Pseudo Code of **CoINR**

---

```

1: Input: INR, Sparsity level, Dictionary size, Random seed
2: Output: Compressed model parameters
3: Initialization:
4:    $\mathbf{A} \leftarrow$  Sample a sensing matrix from  $\mathcal{N}(\mathbf{0}, \mathbf{I})$  using the Random seed
5: for  $layer \in \{2, \dots, l\}$  do
6:   for node in layer do
7:      $\mathbf{w} \leftarrow$  node weights
8:     minimize  $\|\mathbf{x}\|_1$  subject to  $\mathbf{w} = \mathbf{A} \mathbf{x}$ 
9:     indices, values = find( $\mathbf{x} \neq \mathbf{0}$ )
10:   end for
11:   Store nodes’ non-zero indices and values
12: end for
```

---

### A.3 SELECTING THE ACTIVATION FUNCTION

The choice of activation function plays a key role in the performance of an INR, as it is a critical factor in determining its effectiveness. Most of the literature on INR-based compression methods utilizes sinusoidal activations for signal compression. However, this may not always be the most effective activation function for all data modalities. Therefore, in this study, we examined which activation function works best for each data modality.

#### A.3.1 FOR IMAGES

We randomly selected four images from the Kodak dataset to evaluate the image representation capacity of each INR. Figure 8 presents the results alongside the ground truth data. For this evaluation, each INR was configured with 300 hidden neurons. As shown in the results, SIREN consistently outperforms all other INRs; it has been selected for all image compression tasks.

#### A.3.2 FOR OCCUPANCY FIELDS

For the occupancy volumes presented in the main paper, specifically the Stanford Lucy and Thai statue, each occupancy field was trained using different activation functions prior to applying the compression mechanism described in **CoINR**. The performance of each activation was recorded and is summarized in table 1. These experiments were conducted with a hidden neuron count of 128. As shown by the results, Gaussian activation significantly outperforms sinusoidal activation for occupancy volumes. Therefore, it was selected as the default activation function for compressing occupancy volumes.



Figure 8: Image representation performances of different activation functions

Table 1: Occupancy Field Performance Comparison

Occupancy Field	SIREN	GAUSS	WIRE
Thai Statue	0.962	0.975	0.944
Lucy	0.968	0.979	0.965

#### A.4 CHOOSING THE VALUE OF $s$

In this section, we analyze the effect of  $s$  on the performance of the INR across various hidden sizes. We vary the hidden neuron size as 32, 64, 96, 128, 192 and 256. Hidden neuron size of 32 investigates the effect of  $s$  for a 'tiny INR'. From figure 9, we observe that for  $s > 350$ , the performance of the compressed INR closely matches that of the uncompressed INR (denoted by the dotted red line). A similar pattern emerges for other hidden sizes, where performance shows only marginal improvement beyond a certain threshold of  $s$ . This marginal increase typically occurs at an optimal value of  $s$  where **CoINR** achieves sufficient compression. Additionally, we also present a plot which describes the variation of the optimal value of  $s$  with the number of hidden neurons. This plot enables the selection of the optimal  $s$  value for a given hidden size without needing to fit the INR across different values of  $s$ . Notably, the variation of the optimal  $s$  with hidden size is nearly linear.

#### A.5 ADDITIONAL QUALITATIVE, AND QUANTITATIVE RESULTS

In this section, we present the decoded results of **CoINR** and the baseline models for the network configurations  $C_1$ ,  $C_2$ ,  $C_3$ , and  $C_4$ . Additionally, we provide details on the network depth and the number of hidden neurons for each configuration.

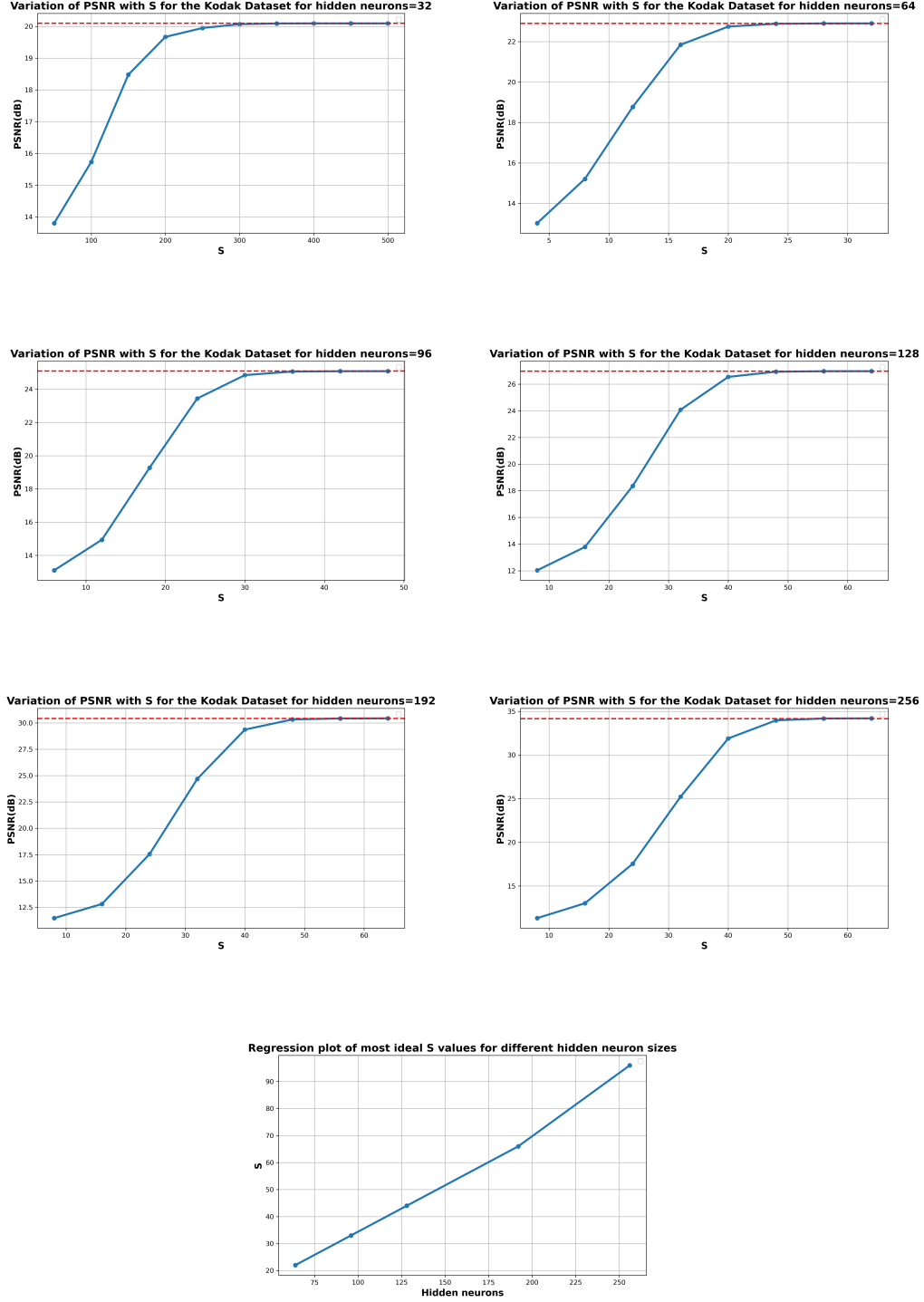


Figure 9: **Variation of PSNR (dB) with the sparsity level for different hidden neurons.** The red dotted line indicates uncompressed INR performance. The regression plot shows that the variation of the optimal value of  $s$  with hidden neuron size is nearly linear.

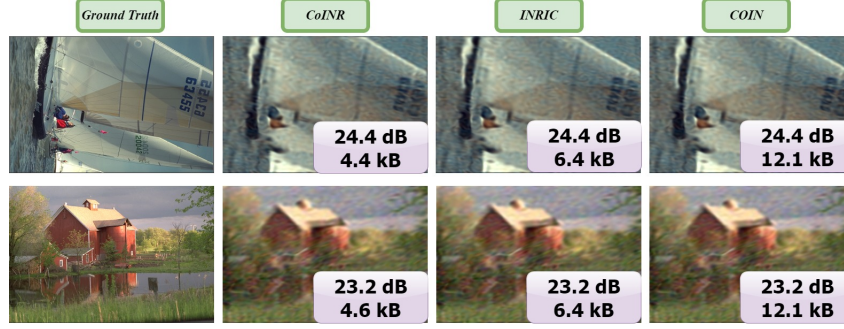


Figure 10: **Image compression performance for configuration  $C_1$  when there are two hidden layers, and 32 neurons:** As can be seen from the results, **CoINR** obtains significant compression compared to baselines

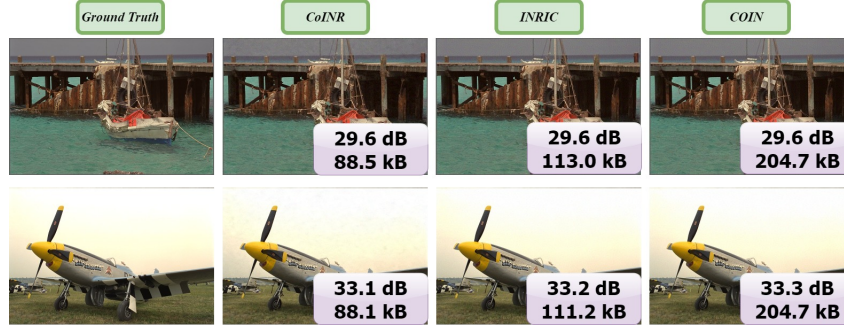


Figure 11: **Image compression performance for configuration  $C_1$  when there are three hidden layers, and 128 neurons:** The results show that **CoINR** achieves significant compression while maintaining the same quantitative metrics as the baselines.

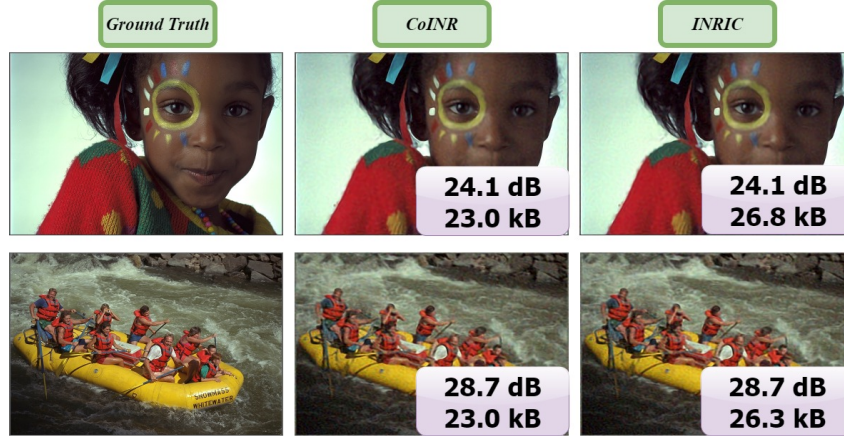


Figure 12: **Image compression performance for configuration  $C_3$  when there are three hidden layers, and 64 neurons:** As can be seen from the results, **CoINR** obtains significant compression while preserving the same quantitative metrics compared to baselines.



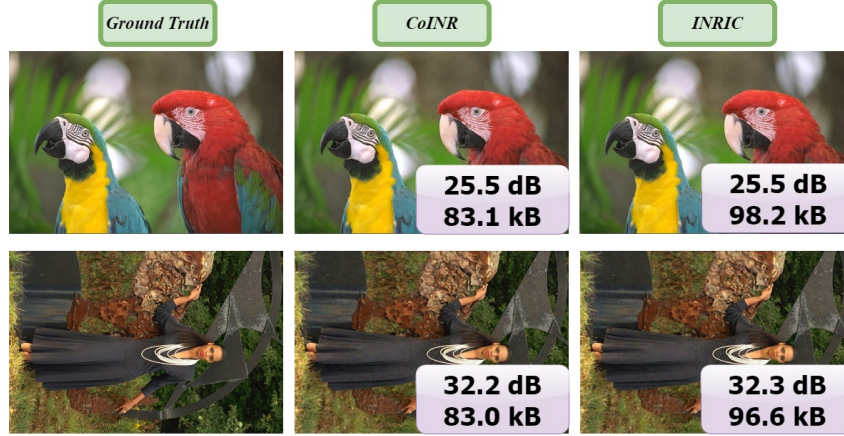


Figure 13: Image compression performance for configuration  $C_3$  when there are three hidden layers, and 128 neurons: The results indicate that CoINR achieves notable compression without compromising the quantitative metrics when compared to the baselines.



Figure 14: Image compression performance for configuration  $C_4$  when there are three hidden layers, and 96 neurons: The results show that CoINR delivers significant compression without compromising quantitative measurements when compared to the baselines.

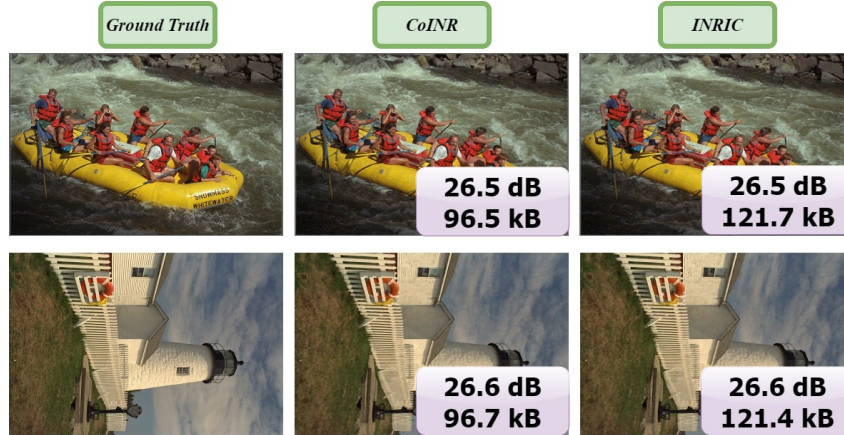


Figure 15: Image compression performance for configuration  $C_4$  when there are three hidden layers, and 128 neurons: The results reveal that CoINR provides significant compression without compromising quantitative measurements when compared to the baselines.